Atomic imprinting in the absence of an intrinsic length scale (F) (SCI)

(iD) Chao Zhou, (iD) Amit Datye, Zheng Chen, (iD) Georg H. Simon, Xinzhe Wang, Jan Schroers, and (iD) Udo D. Schwarz

COLLECTIONS

(F)   This paper was selected as Featured

(SCI)   This paper was selected as Scilight

View Online   Export Citation   CrossMark

Atomic imprinting in the absence of an intrinsic length scale (F) (SCI)

View Online   Export Citation   CrossMark

Chao Zhou,[1] (iD) Amit Datye,[1] (iD) Zheng Chen,[1] Georg H. Simon,[1,a)] (iD) Xinzhe Wang,[1] Jan Schroers,[1] and Udo D. Schwarz[1,2,b)] (iD)

AFFILIATIONS

[1] Department of Mechanical Engineering and Materials Science, Yale University, New Haven, Connecticut 06511, USA
[2] Department of Chemical and Environmental Engineering, Yale University, New Haven, Connecticut 06511, USA

[a)] Present address: Department of Interface Science, Fritz Haber Institute of the Max Planck Society, 14195 Berlin, Germany.
[b)] Author to whom correspondence should be addressed: udo.schwarz@yale.edu

ABSTRACT

Bulk metallic glasses (BMGs) have successfully been used to replicate molds that are structured at the nano- and even atomic scale through thermoplastic forming (TPF), an ability that was speculated to be rooted in the glass' featureless atomic structure. These previous demonstrations of atomically precise imprinting, however, were performed under conditions where mold atomic feature dimensions coincided with the unit cell size of constituents in the BMG. In order to evaluate if accurate atomic-scale replication is possible in general, i.e., independent of the accidental presence of favorable constituent size/feature size relationships, we have used $Pt_{57.5}Cu_{14.7}Ni_{5.3}P_{22.5}$ to replicate three different crystalline facets of $LaAlO_3$ single crystals, each exposing distinct atomic step heights. We find that in all cases, the terraced surface termination can be copied with remarkable fidelity, corroborating that BMGs when thermoplastic formed are capable of adapting to any externally imposed confinement with sub-angstrom precision without being limited by factors related to the specifics of their internal structure. This unprecedented capability of quasi-limitless replication fidelity reveals that the deformation mechanism in the supercooled liquid state of BMGs is essentially homogeneous and suggests TPF of BMGs to be a versatile toolbox for atomic and precision nanoscale imprinting.

INTRODUCTION

Nanostructured and nanopatterned surfaces are an integral component in many nanotechnological applications. Since nanoimprinting offers an avenue to economically produce related products,[1,2] its suitability has been explored related to a wide range of uses, including high-density data storage,[3] photonic devices,[4–6] holograms,[7] bio-nanofluidic chips,[8] sensing,[9,10] manipulation of cellular response,[11,12] water filtration,[13] and electrodes in fuel cells.[14] In order to assess the method's suitability for a specific application, one ought to know the size of the smallest reproducible structural features and the smoothness of the exposed surfaces obtainable with given combinations of materials used for molds and replicas. For certain material combinations, there are intrinsic length scale-related limitations, which have spurred worldwide research efforts into atomic-scale imprinting.[1,11,13,15,16] While

progress has been made in the past, so far, only one idealized case demonstrated sub-angstrom replication fidelity.[17] To establish a universally applicable approach, this paper explores the fundamental limits of nanoimprinting to accurately reproduce a given mold's surface.

Among the different approaches to nanoimprinting, the use of glassy materials as replica materials is particularly promising since they enjoy outstanding processability through thermoplastic forming (TPF) as they soften when heated above their glass transition temperature T_g.[7] From a microscopic perspective, it has been suggested that the room temperature plastic flow that occurs in glassy materials due to externally applied pressure originates from the shear movement of flow units, which are typically referred to as "shear transformation zones" (STZs).[18–24] When the mold feature size decreases and is eventually smaller than that of a flow unit, one would assume an increase in flow resistance to occur

during molding. This ultimately makes the replication of features much smaller than the typical flow unit size of the material more challenging.[25]

For a deeper insight into the mechanisms governing replication fidelity, let us look at a specific example. Despite a room temperature flow unit volume of 123 nm^3 and a chain radius of 0.29 nm,[26,27] polymethyl methacrylate (PMMA), a prototypical glassy polymer, can replicate atomic steps on sapphire through TPF.[15,28] This is possible since at the increased temperatures at which TPF takes place, flow units are much smaller than at room temperature; depending on the temperature at which TPF takes place, they could ideally be as small as individual chains flowing "on their own"—an atomistic picture that is, among other evidence, inspired by the fact that a polymer's viscosity drops above T_g by orders of magnitude. In addition, even if at the temperature where TPF is being performed, there were still flow units with sizes larger than individual chains, these reduced-size flow units (if compared to room temperature) may also more readily alter their shape when exposed to pressure due to the availability of additional thermal energy, shorter relaxation times, and the extra free volume created through thermal expansion, further reducing flow resistance and improving the material's adaptability to confinement.

However, even though the combination of all these factors allows PMMA and other polymers to succeed in replicating features at least two orders of magnitude smaller than both their room temperature flow unit size and their chain length,[16] replication using such materials did not produce any more intricate smaller-scale patterns other than mostly straight steps and the surface terraces on the replica exhibited a roughness noticeably larger than on the mold.[15,16] This remaining limitation likely arises from an entanglement of polymer chains that naturally restricts them how efficiently they flow and pack, thereby effectively preventing "truly homogeneous" flow at the atomic scale. Finally, in the case of PMMA replicating a sapphire surface, overall fidelity was lacking as imprinted step heights were smaller than on the sapphire due to what was assumed to be thermal shrinkage and viscoelastic relaxation.[28]

When looking for a material class likely to overcome such limitations, bulk metallic glasses (BMGs) appear well positioned as room temperature volumes of STZs for BMGs are only a fraction of a nm^3 to several nm^3,[29] i.e., much smaller than for polymers.[30] In addition, the relative atomic structure of BMGs can be flexibly rearranged with the size and packing density of the atoms themselves as the only limiting factors. At temperatures sufficiently above T_g, this may result in an ideally homogeneous flow that allows the material to adapt to any externally imposed confinement. For proof of concept, a $Pt_{57.5}Cu_{14.7}Ni_{5.3}P_{22.5}$ BMG alloy has been used that exhibits excellent ductility, plasticity, and thermoplastic formability as well as a conveniently long processing window without suffering from excessive oxidation or
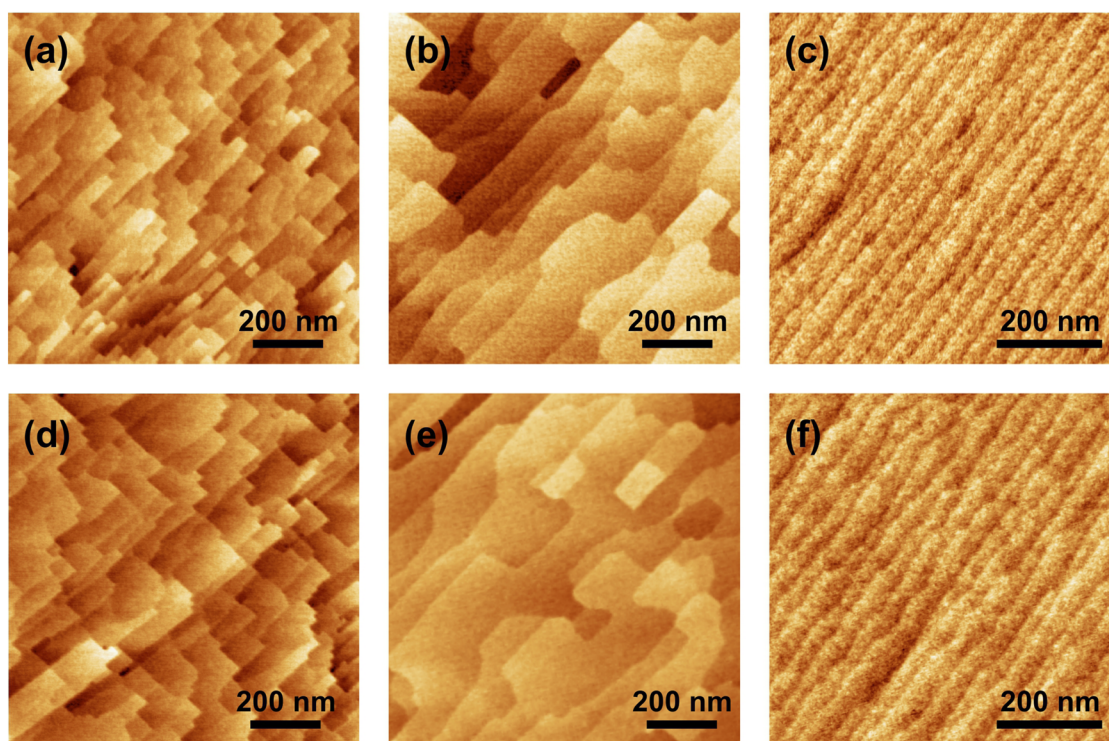
FIG. 1. AFM images in (a)–(c): LaAlO$_3$ (100), (110), and (111) surfaces after thermoplastic forming. [(d)–(f)] Mirrored and z-inverted AFM images of the corresponding Pt-BMG replica revealing their imprinted features. In all three cases, the characteristic surface features exposed by the molds are accurately reproduced.

premature crystallization at conditioning temperatures.[31] Thermoplastically pressing this BMG onto strontium titanate (SrTiO$_3$) replicated the crystal's step edges with atomic precision and high fidelity while preserving the smoothness of its terraces with a ≈0.060 nm root mean square (rms) roughness[17] even though the size of an STZ at room temperature of Pt-BMG was reported to be approximately several nm^3, which contains several hundreds of atoms.[29]

Returning to the original question of maximum imprinting accuracy, the success of this proof-of-concept suggests that the limit of replication fidelity that can be achieved by TPF with BMGs can go *beyond the scale of their flow unit size*, which ultimately may be the size of a single atom. In the above case, however, the step height between terraces of SrTiO$_3$(100) is 0.3905 nm,[32] a value that diverges less than 0.2% from the lattice constant of the BMG's majority chemical compound, platinum, of 0.3912 nm.[33] Thus, it is valid concern to wonder whether or not the precise replication of SrTiO$_3$(100) using an Pt$_{57.5}$Cu$_{14.7}$Ni$_{5.3}$P$_{22.5}$ alloy may simply be owed (or at least facilitated) to the coincidental quasi-match of the mold's lattice constant with the one of platinum.

In this research, it is shown that atomic imprinting via TPF can be generalized to the replication of surfaces with different characteristic dimensions. For this case study, we use the (100), (110), and (111) surfaces of lanthanum aluminate (LaAlO$_3$), all of which offer different step heights and surface features such as screw dislocations that despite their complexity can be reproduced without loss of resolution. From these results, we infer that bulk metallic glasses may indeed not possess an apparent intrinsic length scale limiting the accuracy of atomic feature replication through TPF, thereby providing an ideal platform for advancing research in the fundamental study of structure, deformation, and phase transitions of glasses[34,35] as well as enabling novel applications in fields that make use of surface functionalization through topography.[25,36]

MATERIALS AND METHODS

LaAlO$_3$ (100), (110), and (111) single crystals with one side polished were bought from MTI Corporation (Richmond, CA, USA). The surfaces were cleaned by wet etching in dilute HCl with the pH value near 4.5 for 30 s. The crystalline surface was then annealed at 1050 °C in air for 10 h.[37] Thermoplastic forming was conducted using an Instron 5569 mechanical testing machine with custom heating plates as follows: A cylindrical ingot of an amorphous Pt$_{57.5}$Cu$_{14.7}$Ni$_{5.3}$P$_{22.5}$ alloy ("Pt-BMG")[31] ~2 mm in length and 1 mm in diameter that was produced by casting was thermoplastically formed onto LaAlO$_3$ substrates at constant force and temperature. After a thermal equilibrium at a temperature of 270 °C was achieved, the force was ramped up to a maximum value of 1 kN (≈10 MPa) that was maintained for about 3 min. The sample was then air cooled to ambient temperature. Details of the TPF procedure can be found in previous publications.[17,38]

The surfaces of the LaAlO$_3$ molds and Pt-BMG replicas were characterized with atomic force microscopy (AFM) using a Bruker Multimode AFM with Nanoscope III electronics and Bruker RTESPAW-300 cantilevers with driving frequencies around 300 kHz in tapping mode. Following a protocol developed previously,[17] the original AFM images of as-imprinted Pt-BMG were mirrored along the y–z plane followed by inverting the image's z-scale in order to

facilitate direct comparison between the surface morphologies of mold and replica.

RESULTS AND DISCUSSION

At room temperature, single crystalline LaAlO$_3$ has a rhombohedral structure, which can be simplified as a pseudo-cubic structure with $a = b = c = 0.3787$ nm and $\alpha = 90.066°$.[39,40] Thus, step heights between individual terraces on LaAlO$_3$ (100), (110), and (111) are integer multiples of ≈0.38 nm, ≈0.27 nm, and ≈0.22 nm, respectively. Similar to other perovskite oxides, LaAlO$_3$ surfaces exhibit under ultra-high vacuum conditions a variety of surface reconstructions.[41,42] The combined effects of orientation, miscut, and preparation-dependent surface termination led to surface patterns that are, at least for the samples investigated in this study, distinct for LaAlO$_3$ (100), (110), and (111) surfaces: while the (100) surface [Fig. 1(a)] shows terraces with relatively sharp corners, the step edges separating individual terraces on LaAlO$_3$(110) [Fig. 1(b)] tend to be more rounded. There are also more island-like and pit-like features on the (110) surface, which may be a consequence of this particular crystal's lower miscut compared to the one of Fig. 1(a). In contrast, the surface of the LaAlO$_3$(111) single crystal is not only exhibiting the largest miscut of the three samples, but it was also prone to degradation. Thus, rather than observing a more fine-structured pattern with step edges
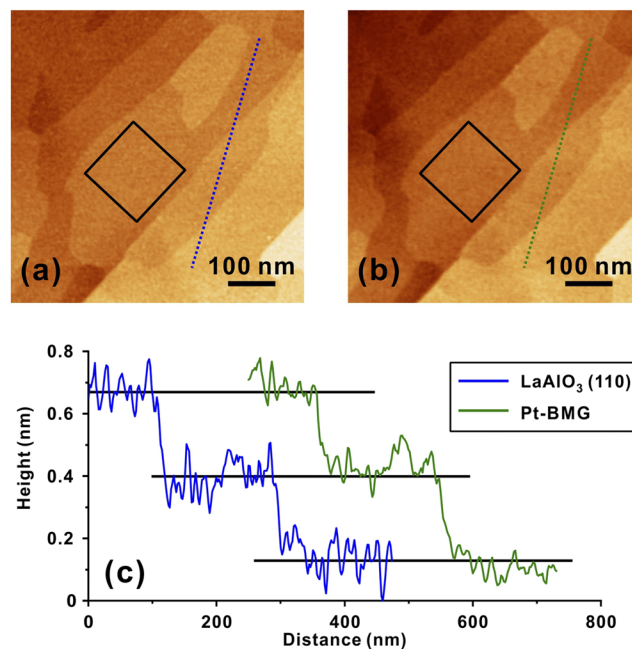
FIG. 2. Replication of LaAlO$_3$(110) onto Pt-BMG. (a) AFM image of the LaAlO$_3$(110) surface after thermoplastic forming and (b) mirrored and z-inverted AFM image of the corresponding location on the Pt-BMG replica, revealing the exact same surface features as observed in (a). (c) Line profiles taken along the direction indicated by the blue and green dotted lines in (a) and (b), exposing identical step heights of 0.27 nm on both the mold and the replica. The areas marked by the squares possess an rms roughness of (a) 0.065 nm and (b) 0.055 nm, respectively.
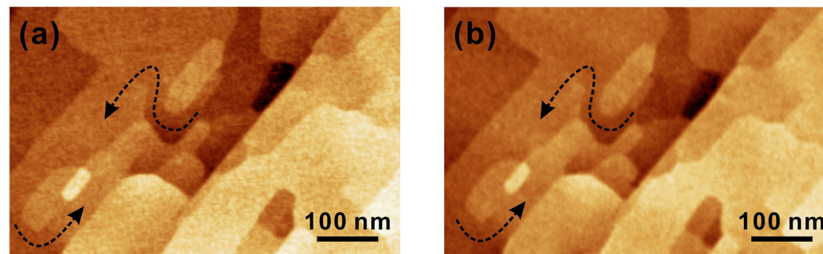
FIG. 3. Replication of screw dislocations on the LaAlO$_3$(110) surface onto BMG. (a) AFM image of LaAlO$_3$(110) after thermoplastic forming. (b) Mirrored and z-inverted AFM image of BMG. The height of terraces continuously increases along the dashed lines with arrows by one unit cell (0.27 nm), which is caused by two screw dislocations terminating at the surface. The points where the step edges emerge from, which mark the sites where the screw dislocation lines intersect with the surface, are located near the positions of the arrow heads.

exhibiting frequent kinks, only continuous and dense steps were observed that separated terraces showing significantly higher roughness than on the other two samples [Fig. 1(c)]. Nevertheless, the step heights between terraces matched the theoretical values for all three samples.

Moving forward, the distinctively different surface patterns exposed by the crystals combined with their well-defined step heights provide ideal references for assessing the fidelity of feature replication through thermoplastic forming when using them as comparative molds. Without loss of generality, Figs. 1(d)–1(f) present AFM images of the morphology of the respective nanoimprinted surfaces using Pt-BMG after mirroring and z-inversion, where all three expose the same signature features and step heights found on the corresponding LaAlO$_3$ molds. Despite the abovementioned increased on-terrace roughness, the replication of the LaAlO$_3$(111) surface demonstrates the capability to fabricate feature sizes down to 0.22 nm using Pt-BMG.

To highlight an exemplary case in more detail, we quantified the replication quality through surface roughness analysis and comparison of line profiles across terraces using LaAlO$_3$(110). Toward this end, Fig. 2(a) shows the mold LaAlO$_3$(110) surface after thermoplastic forming, while Fig. 2(b) was taken at the corresponding location on the imprinted Pt-BMG. After mirroring and z-inversion, we can easily see that it indeed shows the exact same features as the mold. For the roughness analysis, we use the areas within the squares shown in Figs. 2(a) and 2(b), which are 150 × 150 nm^2 in size each. Computing the root mean square (rms) roughness results in values of 0.065 nm and 0.055 nm, respectively, with the slight difference possibly being due to the probing tips exposing differently sharp apexes. In any event, the observed surface roughness matches previously reported results on SrTiO$_3$, indicating that Pt-BMG also has favorable wetting properties toward the LaAlO$_3$ surface.[17] The line profiles in Fig. 2(c) then demonstrate the accurate replication of the 0.27 nm height of the step edges. As a result, we conclude that nanoimprinting Pt-BMG onto LaAlO$_3$ crystals achieves the same quality as obtained when using SrTiO$_3$ as molds.

Compared to the LaAlO$_3$ (100) and (111) surface terminations, the (110)-terminated LaAlO$_3$ crystal was exhibiting more complex atomic-scale features originating from defects such as screw dislocations, which can provide additional insight when evaluating the scale limit of atomic imprinting. For example, the surface area

presented in Fig. 3(a) exposes two screw dislocations terminating at the surface, which are highlighted by two dashed lines with arrows; Fig. 3(b) reflects the corresponding structure in the Pt-BMG replica. Following the dashed lines along the direction of the arrow, one can seamlessly move from a lower terrace to a higher one, while the step edge emerges from the point where the screw dislocation line intersects with the surface. Since the nature and appearance of screw dislocations at surfaces have been investigated in detail elsewhere,[43] we only note here that the successful replication of such a continuously changing feature corroborates again that there is likely no intrinsic scale limit to the accuracy of thermoplastically replicating the height of surface features with suitable BMGs even at the atomic scale.

More generally, TPF is found to be capable of replicating most or all features that are resolvable by AFM, which is sub-angstrom in the z direction and, due to the finite radius of the probing tip, a couple of nanometers laterally during ambient air imaging. As a result, it provides an ideal platform to study local glass transition kinetics at the nanometer scale. For example, previous research has shown that the change in surface morphology during sequential annealing of imprinted Pt-BMG replica using SrTiO$_3$(100) as mold results from the competition between surface relaxation and crystallization.[35] Thereby, the smoothening of the steps is due to the surface relaxation, while the roughening on the terraces is because of the onset of crystallization starting first near the surface. Through the purposeful selection of surfaces employed as molds, we can generate BMG replicas with different step heights. Subsequently, we could get an estimation of the time scale for surface and bulk relaxation by pinpointing the temperatures and annealing times at which steps with different heights flatten out.

CONCLUSIONS

In this research, we demonstrated the nanoimprinting of Pt-BMG by LaAlO$_3$ surfaces with atomic-scale replication fidelity through TPF. Particular emphasis was given to the reproduction of patterns with clearly defined but different characteristic dimensions, which was achieved through the use of LaAlO$_3$ single crystals with three different crystallographic surface orientations. Surfaces on these crystals then expose terraces separated by distinct but different step heights, all of which were replicated with sub-angstrom

precision. Together with the impeccable replication of screw dislocations on LaAlO$_3$(110), which feature continuously changing terrace heights near the point where the dislocation line hits the surface, the results indicate that there may indeed not be an intrinsic scale limiting the ability of BMGs to accurately replicate the heights of surface features on molds by TPF. This presumed "ultimate" imprinting capability of TPF with BMGs not only broadens the application of TPF in atomic imprinting and precision nanofabrication but also offers a material system that allows us to continuously tune the size of surface features for fundamental high-resolution and local studies of glass properties and behavior.

ACKNOWLEDGMENTS

DATA AVAILABILITY

The data that support the findings of this study are available from the corresponding author upon reasonable request.

REFERENCES

[1] Y. S. Chou, *Nanofabrication Handbook*, 1st ed., edited by S. Cabrini and S. Kawata (CRC Press, 2012), Chap. 9.

[2] S. Y. Chou, P. R. Krauss, and P. J. Renstrom, Science **272**(5258), 85–87 (1996).

[3] P. R. Krauss and S. Y. Chou, Appl. Phys. Lett. **71**(21), 3174–3176 (1997).

[4] P. Nagpal, N. C. Lindquist, S.-H. Oh, and D. J. Norris, Science **325**(5940), 594–597 (2009).

[5] C. Zhang, H. Subbaraman, Q. Li, Z. Pan, J. G. Ok, T. Ling, C.-J. Chung, X. Zhang, X. Lin, R. T. Chen, and L. J. Guo, J. Mater. Chem. C **4**(23), 5133–5153 (2016).

[6] Z. Yu, P. Deshpande, W. Wu, J. Wang, and S. Y. Chou, Appl. Phys. Lett. **77**(7), 927–929 (2000).

[7] J. Schroers, Adv. Mater. **22**(14), 1566–1597 (2010).

[8] X. Chen and L. Zhang, Sens. Actuators, B **254**, 648–659 (2018).

[9] E. R. Kinser, J. Padmanabhan, R. Yu, S. L. Corona, J. Li, S. Vaddiraju, A. Legassey, A. Loye, J. Balestrini, D. A. Solly, J. Schroers, A. D. Taylor, F. Papadimitrakopoulos, R. I. Herzog, and T. R. Kyriakides, ACS Sens. **2**(12), 1779–1787 (2017).

[10] S. Zhang, C. Zhang, H. Chen, S. J. Kieffer, F. Neubrech, H. Giessen, A. G. Alleyne, and P. V. Braun, Angew. Chem., Int. Ed. **58**(50), 18165–18170 (2019).

[11] J. Padmanabhan, E. R. Kinser, M. A. Stalter, C. Duncan-Lewis, J. L. Balestrini, A. J. Sawyer, J. Schroers, and T. R. Kyriakides, ACS Nano **8**(5), 4366–4375 (2014).

[12] A. M. Loye, E. R. Kinser, S. Bensouda, M. Shayan, R. Davis, R. Wang, Z. Chen, U. D. Schwarz, J. Schroers, and T. R. Kyriakides, Sci. Rep. **8**(1), 8758 (2018).

[13] L. M. Cox, A. M. Martinez, A. K. Blevins, N. Sowan, Y. Ding, and C. N. Bowman, Nano Today **31**, 100838 (2020).

[14] R. C. Sekol, G. Kumar, M. Carmo, F. Gittleson, N. Hardesty-Dyck, S. Mukherjee, J. Schroers, and A. D. Taylor, Small **9**(12), 2081–2085 (2013).

[15] G. Tan, N. Inoue, T. Funabasama, M. Mita, N. Okuda, J. Mori, K. Koyama, S. Kaneko, M. Nakagawa, A. Matsuda, and M. Yoshimoto, Appl. Phys. Express **7**(5), 055202 (2014).

[16] S. Elhadj, R. M. Rioux, M. D. Dickey, J. J. DeYoreo, and G. M. Whitesides, Nano Lett. **10**(10), 4140–4145 (2010).

[17] R. Li, Z. Chen, A. Datye, G. H. Simon, J. Ketkaew, E. Kinser, Z. Liu, C. Zhou, O. E. Dagdeviren, S. Sohn, J. P. Singer, C. O. Osuji, J. Schroers, and U. D. Schwarz, Commun. Phys. **1**(1), 75 (2018).

[18] A. S. Argon, Acta Metall. **27**(1), 47–58 (1979).

[19] P. Schall, D. A. Weitz, and F. Spaepen, Science **318**(5858), 1895–1899 (2007).

[20] W. H. Wang, J. Appl. Phys. **110**(5), 053521 (2011).

[21] N. Li, W. Chen, and L. Liu, JOM **68**(4), 1246–1261 (2016).

[22] F. Spaepen, Scr. Mater. **54**(3), 363–367 (2006).

[23] Y. Zhang and A. L. Greer, Appl. Phys. Lett. **89**(7), 071907 (2006).

[24] A. L. Greer, Y. Q. Cheng, and E. Ma, Mater. Sci. Eng., R **74**(4), 71–132 (2013).

[25] G. Kumar, H. X. Tang, and J. Schroers, Nature **457**(7231), 868–872 (2009).

[26] A. Samadi-Dooki, L. Malekmotiei, and G. Z. Voyiadjis, Polymer **82**, 238–245 (2016).

[27] L. Malekmotiei, A. Samadi-Dooki, and G. Z. Voyiadjis, Macromolecules **48**(15), 5348–5357 (2015).

[28] M. Yoshimoto, Appl. Phys. A **121**(2), 321–326 (2015).

[29] D. Pan, A. Inoue, T. Sakurai, and M. W. Chen, Proc. Natl. Acad. Sci. U. S. A. **105**(39), 14769–14772 (2008).

[30] Y. Ma, G. J. Peng, T. T. Debela, and T. H. Zhang, Scr. Mater. **108**, 52–55 (2015).

[31] J. Schroers and W. L. Johnson, Appl. Phys. Lett. **84**(18), 3666–3668 (2004).

[32] A. Okazaki and M. Kawaminami, Mater. Res. Bull. **8**(5), 545–550 (1973).

[33] W. P. Davey, Phys. Rev. **25**(6), 753–761 (1925).

[34] Z. Chen, A. Datye, P. A. Brooks, M. Sprole, J. Ketkaew, S. Sohn, J. Schroers, and U. D. Schwarz, MRS Adv **4**(2), 73–79 (2019).

[35] Z. Chen, A. Datye, J. Ketkaew, S. Sohn, C. Zhou, O. E. Dagdeviren, J. Schroers, and U. D. Schwarz, Scr. Mater. **182**, 32–37 (2020).

[36] M. Hasan, J. Schroers, and G. Kumar, Nano Lett. **15**(2), 963–968 (2015).

[37] A. Biswas, C.-H. Yang, R. Ramesh, and Y. H. Jeong, Prog. Surf. Sci. **92**(2), 117–141 (2017).

[38] G. Kumar, P. A. Staffier, J. Blawzdziewicz, U. D. Schwarz, and J. Schroers, Appl. Phys. Lett. **97**(10), 101907 (2010).

[39] S. Geller and V. B. Bala, Acta Crystallogr. **9**(12), 1019–1025 (1956).

[40] G. W. Berkstresser, A. J. Valentino, and C. D. Brandle, J. Cryst. Growth **109**(1-4), 467–471 (1991).

[41] Z. L. Wang and A. J. Shapiro, Surf. Sci. **328**(1-2), 141–158 (1995).

[42] K. Krishnaswamy, C. E. Dreyer, A. Janotti, and C. G. Van de Walle, Phys. Rev. B **90**(23), 235436 (2014).

[43] J. Engbaek, J. Schiotz, B. Dahl-Madsen, and S. Horch, Phys. Rev. B **74**(19), 195434 (2006).